Optical Engineering

OpticalEngineering.SPIEDigitalLibrary.org

Quantitative measurement of CO_2 laser-induced residual stress in fused silica optics

Liang Yang
Wei Liao
Xinxiang Miao
Xiaodong Yuan
Wanguo Zheng
Haibin Lv
Guorui Zhou
Xiaotao Zu
Xia Xiang

SPIE.

Quantitative measurement of CO_2 laser-induced residual stress in fused silica optics

Liang Yang,[a,b] Wei Liao,[a,*] Xinxiang Miao,[a] Xiaodong Yuan,[a] Wanguo Zheng,[a] Haibin Lv,[a] Guorui Zhou,[a] Xiaotao Zu,[b] and Xia Xiang[b,*]
[a]Research Center of Laser Fusion, China Academy of Engineering Physics, Mianyang 621900, China
[b]University of Electronic Science and Technology of China, School of Physical Electronics, Chengdu 610054, China

Abstract. The residual stress field of fused silica induced by continuous wave CO_2 laser irradiation is investigated with specific photoelastic methods. Both hoop stress and axial stress in the irradiated zone are measured quantitatively. For the hoop stress along the radial direction, the maximum phase retardance of 30 nm appears at the boundary of the laser distorted zone (680-μm distance to center), and the phase retardance decreases rapidly and linearly inward, and decreases slowly and exponentially outward. For the axial stress, tensile stress lies in a thin surface layer (<280 μm) and compressive stress lies just below the tensile region. Both tensile and compressive stresses increase first and then decrease along the depth direction. The maximum phase retardance induced by axial tensile stress is 150 nm, and the maximum phase retardance caused by axial compression stress is about 75 nm. In addition, the relationship between the maximum axial stress and the deformation height of the laser irradiated zone is also discussed. [DOI: 10.1117/1.OE.54.5.057105]

Keywords: fused silica; CO_2 laser; hoop stress; axial stress.

Paper 150311 received Mar. 11, 2015; accepted for publication Apr. 20, 2015; published online May 8, 2015.

1 Introduction

Due to its excellent transmission performance in the ultraviolet (UV) band, fused silica is used as one of the most important optical materials in many high-fluence and high-peak power laser facilities. In particular, it serves as beam-transport lenses and vacuum windows for the large laser facilities such as the National Ignition Facility in the USA,[1] the Laser Megajoule in France,[2] and the SG-III laser facility in China.[3] The lifetime of fused silica components under UV laser irradiation has been extensively investigated and the results show that the lifetime of fused silica optics is determined by both surface damage initiation and damage growth.[4–6] Hence, in order to prolong the lifetime of optics and reduce the operating costs, several methods have been developed to mitigate the damage growth of optics, including wet chemical etching, cold plasma etching, microflame torch processing, CO_2 laser processing, and so on.[7] Among these mitigation methods, continuous wave CO_2 laser processing exhibits the most consistent and convincing results for mitigating the growth of heavily damaged fused silica. Moreover, the CO_2 laser processing method is inexpensive and straightforward to apply for mitigating sites on large optics.[8] However, it is known that residual stress may be generated around the mitigated sites after CO_2 laser irradiation, which could cause critical fractures either during or after laser treatment.[9] Therefore, it is necessary to have a good understanding of the residual stress behaviors of fused silica induced by the CO_2 laser process. Some research has already been done on this subject.

The formation mechanism of the residual stress by CO_2 laser irradiation has been studied.[10–12] The general explanation of the formation of the residual stress involves three steps: (a) temperature gradient formed at the initial stage of irradiation, (b) thermal expansion during laser irradiation due to the positive thermal expansion coefficient of fused silica, and (c) elastic and plastic deformation appearing after the lasers are turned off. Several numerical models have also been presented to simulate the evolution of the fictive temperature and stress field with the finite element method,[9,13–15] such as tool-Narayanaswamy relaxation model,[9] elastoviscoplastic deformation model,[13] and thermomechanical model.[14,15] In addition, several methods have been developed to characterize the mitigated area. For instance, Matthews et al.[9] characterized the thermal stress regions using polarimetry and confocal Raman microscopy to measure the stress-induced birefringence and fictive temperature. Guignard et al.[10] studied the residual stress of fused silica and K9 glass with microscopic observations and an interferometric method. Gallais et al.[15] investigated the residual stress field created around mitigated sites with photoelastic method. The correlation between the place where the damage occurs and the location of the maximal residual stress was also investigated.[15,16]

The previous studies mainly focused on the production mechanism of the residual stress by theoretical analysis, the evolution process of stress field by numerical simulation, and the correlation between laser parameters and residual stress and how to eliminate the stress from optics by experiments. Little work has been done to quantitatively measure the residual stress itself in the irradiated region induced by the CO_2 laser. Hence, it is necessary to experimentally investigate the distribution of the stress field, which is helpful for understanding the residual stress behaviors.

In this paper, the residual stress distribution of fused silica is investigated by a stress analyzer after 10.6 μm CO_2 laser

*Address all correspondence to: Wei Liao, E-mail: benleo4job@163.com; Xia Xiang, E-mail: xiaxiang@uestc.edu.cn

irradiation. The hoop stress and axial stress in the irradiated zone are measured to obtain the location of the maximum stress and the distribution of the residual stress in the irradiated region. Since fused silica is a transparent material, a photoelastic method is chosen to measure the phase retardance data, which is proportional to the magnitude of the localized stress. In addition, the mechanism of residual stress formation during and after laser mitigation is also discussed.

2 Experimental Result

2.1 *Sample Preparation and Damage Sites Generation*

Optically polished fused silica glass (Corning 7980) with the dimensions of $30 \times 30 \times 10$ mm^3 was used in this paper. Before the experiments, the sample was etched for 10 min in a buffered HF solution ($1\%HF + 15\%NH_4F + 84\%H_2O$) in order to remove the surface contaminations and blunt the subsurface scratches. Then the sample was cleaned immediately with highly pure water and alcohol after etching. The damage sites with a diameter of 200 μm were generated by a single longitudinal mode Q-switched Nd:YAG laser, which operated at 355 nm with a pulse width of 6.3 ns.

2.2 CO_2 *Laser Mitigation Procedure*

A radio frequency excited CO_2 laser (Coherent GEM-100L) was used to mitigate the damage sites. The mode of the CO_2 laser is TEM00 (>95%) and the laser operates at 10.6 μm with an approximately spatially Gaussian profile. A ZnSe lens with a focal length of 10 cm was used to focus the CO_2 laser beam on the damage sites. The diameter of a focal spot at the sample surface is about 4 mm at $1/e^2$ as measured by the knife-edge method. The laser energy is monitored by an EPM1000 energy meter and was adjusted by changing the duty ratio of the laser. In addition, a visible He–Ne probe beam coaxial with a CO_2 laser was used for collimation to make sure the repair region could be accurately located. A scientific CCD camera is used to monitor the repair process.

The repair parameters have been optimized before this experiment, including the size of damage site (L), diameter of the CO_2 laser spot (D), laser power (P), irradiation time (t), and shot number (N), which are listed in Table 1. The morphology of the damage site and the irradiated zone was measured by an optical microscope, as shown in Fig. 1. The repair profile indicates that the damaged site was completely melted and smoothed after CO_2 laser treatment.

2.3 *Stress Measurement*

In this paper, the Senarmont compensated method and sensitive color method are used to characterize the residual stress distribution of the repaired region by a PTC-720 stress analyzer, which is based on the property of birefringence that is exhibited by certain transparent materials under stress.

Table 1 Repair parameters of the damage sites.

L (μm)	D (mm)	P (W)	t (s)	N
200	4	23	12	2

The Senarmont compensated method can quantitatively measure the value of the phase retardation with a deviation less than ± 1.5 nm The sensitive color method is extremely intuitive for observing the stress. The background color in the visual field is purple, which is called the "photosensitive color." Yellow or saffron yellow represents the tensile stress, while green or blue represents the compressive stress existing in the sample. The basic principle and more details have been described elsewhere.[17]

In order to investigate the stress distribution in the irradiated zone, both hoop stress and axial stress were studied and the pictures are shown in Figs. 2–5. The residual stress cannot be easily obtained because it may be distributed as a function of depth. Nevertheless, phase retardation, which is proportional to the localized stress, can be measured quantitatively, so phase retardation is used to characterize the stress. The phase retardation data (R) can be converted to stress (σ) according to Eq. (1) if the optical path length (L) and photoelastic constant (C) of the transparent sample are known

$$\sigma(\mathrm{MPa}) = \frac{R(\mathrm{nm})}{C(\mathrm{kg/cm^2}) \times L(\mathrm{cm})}. \quad (1)$$

In this paper, phase retardation along the radial direction and along the depth direction were measured quantitatively by the Senarmont compensated method, as shown in Figs. 3 and 5. The compressive stress is set as a negative valve and the tensile stress is set as a positive value.

3 Results and Discussion

3.1 *Hoop Stress*

Figure 2 shows the hoop stress generated around the mitigated site. The stress distribution image in Fig. 2(a) was measured by the Senarmont compensated method and that in Fig. 2(b) was measured by the sensitive color method. The results show that both tensile and compressive stresses were generated after CO_2 laser irradiation. A maximum stress is evidenced around the mitigated crater, and the stress distribution is axially symmetrical. The phase retardation distribution of the mitigated site along the radial direction is shown in Fig 3. It reveals that the maximum of the phase retardance appeared at a 680-μm distance from the beam center, and the phase retardance decreases rapidly and linearly inward, and decreases slowly and exponentially outward. This trend is similar to the report described in Ref. 15, However, they did not quantitatively measure the phase retardance.

In order to understand why the maximum phase retardance located near the boundary of the mitigated crater, the morphology of the mitigated site created by CO_2 laser irradiation should be studied. The top view of the mitigated crater is shown in Fig. 1(b). The side view of the mitigated crater is shown in Fig. 1(c). The microscopic morphologies indicate that the surface of fused silica is distorted after CO_2 processing. The irradiated area can be divided into the distorted zone and the laser affected zone.[12] The red dotted circle in Fig. 1(b) is the boundary of the laser distorted zone. The radius of the circle is about 680 μm. Thus, the diameter of the location where the maximum phase retardance occurred nearly equals the diameter of the laser distorted zone. Thus, the maximum hoop stress is located at

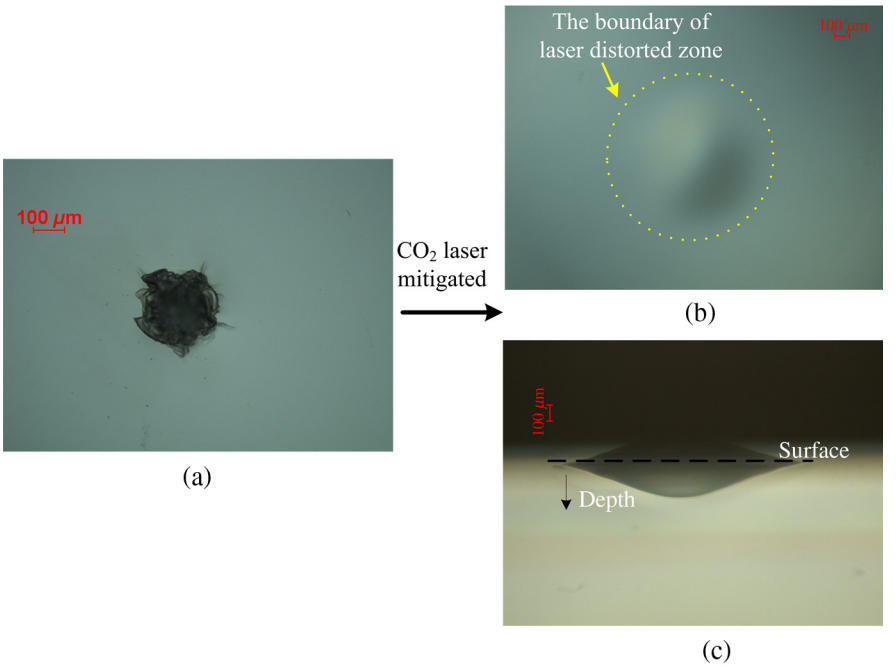

Fig. 1 Optical microscopic images: (a) damage site, (b) mitigated site in top view, and (c) mitigated site in side view.

the boundary of the laser distorted zone. Therefore, a conclusion can be made that material deformation would cause stress generation and the maximum stress usually appears in the boundary of the laser distorted zone. Due to the low thermal conductivity of the fused silica at room temperature, the temperature gradient between the laser irradiated area and the surrounding area is very large. The maximum temperature gradient may occur on the boundary of the laser distorted area, which may be the main reason for the maximum hoop stress appearing in this zone.

3.2 *Axial Stress*

3.2.1 *Axial stress along the depth direction*

Figure 4 shows the axial residual stress generated in the surface layer of fused silica. The axial stress distribution is measured by the Senarmort compensated method [Fig. 4(a)] and the sensitive color method [Fig. 4(b)], respectively. The results show that tensile stress lies in a thin surface layer and the compressive stress lies just below the tensile region. This experimental result is in accordance with the numerically simulated result in Ref. 9. The thermal stress occurs due to the temperature gradient in the laser heated region. Some studies have explained this phenomenon.[8–10,15] The absorption of the CO_2 laser radiation leads to the heating of a thin surface layer which induces thermal stress. As long as temperature remains below the glass transition temperature, the glass behaves as an elastic material. At higher laser fluence, the temperature increases above the glass transition temperature, so the glass becomes a viscous liquid and the stress relaxes. After the laser turns off, the viscosity rapidly increases when the material temperature cools down to

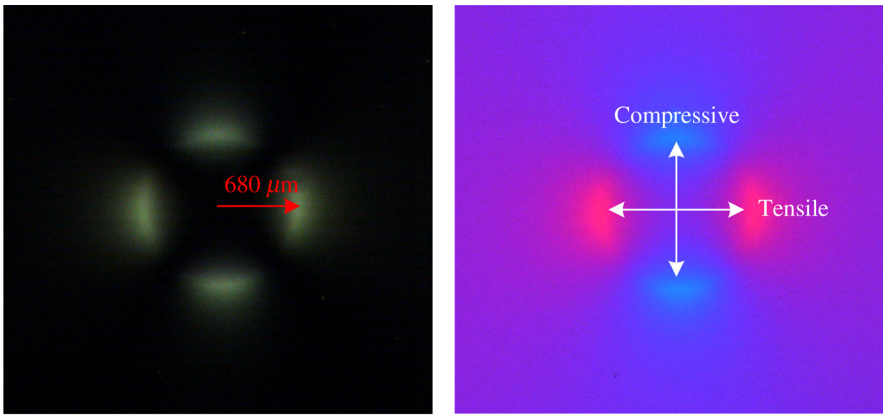

Fig. 2 Hoop stress around mitigated site measured by (a) the Senarmort compensated method and (b) the sensitive color method with stress analyzer.

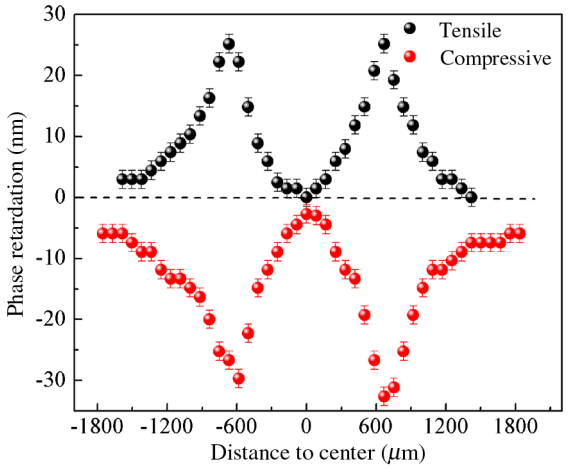

Fig. 3 Phase retardation distribution of the mitigated site along the radial direction.

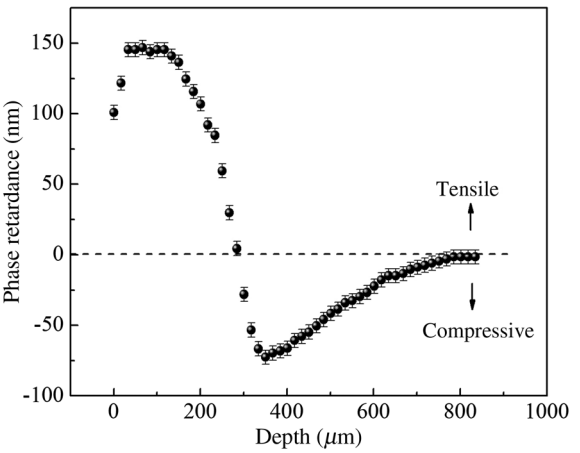

Fig. 5 Phase retardance distribution of the mitigated site in the beam center along the depth direction.

the ambient temperature. Stress cannot be released during the rapid cooling process, So residual tensile stress remains in the thin surface layer. At the same time, a small region with compressive stress is developed just below the tension region because the surrounding material cools and restricts the flow of the viscous material.

In order to investigate the distribution of the axial residual stress, the phase retardance along the axial direction is measured. For the sake of easy description, the coordinates in Fig. 4(a) are set up. The origin of the coordinate should coincide with the beam center. The r-axis is vertical to the laser propagation direction and the z-axis is parallel to the laser propagation direction. As for $r = 0$, the distribution of the axial stress in the beam center along the depth direction can be obtained by measuring the phase retardation along the z-axis, and the result is shown in Fig. 5. The result indicates that the phase retardation is positive, which correlates with the tensile stress when $z < 280$ μm, then it becomes negative, which correlates with the compressive stress when 280 μm $< z <$ 850 μm. In other words, the phase retardation is zero when z is equal to 280 μm, which is the boundary of tensile stress and compressive stress. In addition, the axial stress curve also reveals that the maximum tensile stress is not located at the surface, but is 50 to 100 μm below the surface. The maximum of phase retardation reaches to 150 nm, which is why the cracks initiate in the subsurface of the sample after CO_2 laser irradiation.[9,10] The maximum compression stress is located at a depth of 320 μm from surface and the absolute value of the maximum phase retardation is about 75 nm. These compression stresses will stop fractures propagating inside the glass.[10]

3.2.2 *Relationship between maximum axial stress and deformation height*

In order to understand the relationships between maximum axial stress and deformation height of the laser irradiated zone, the surface profile of the mitigated craters and the distribution of the phase retardation in the irradiated zone should be investigated. In this paper, a stylus profilometry (Ambios XP-Plus 300) is used to obtain the surface profile of the mitigated craters. Figure 6 shows the stylus profilometry trace of the crater and it is near Gaussian. The phase retardation of the location (r, z) is set as $R(r, z)$. In the irradiated zone, the phase retardation along z was measured for each r. Then the maximum of the positive data for each r was extracted to constitute the maximum tensile stress curve. The minimum of the negative data for each r was extracted to constitute the maximum compressive stress curve, and the results are shown in Fig. 7. The curves reveal that the distribution of the both tensile stress and compressive stress is near Gaussian profile. Therefore, either tensile stress or compressive stress is proportional to the deformation height of the laser irradiated zone.

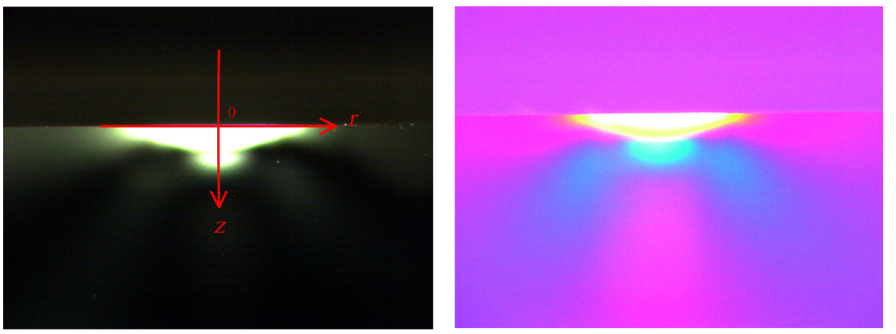

(a) (b)

Fig. 4 Axial stress distributions of the mitigated site measured by (a) the Senarmort compensated method and (b) the sensitive color method with polarizer stress analyzer.

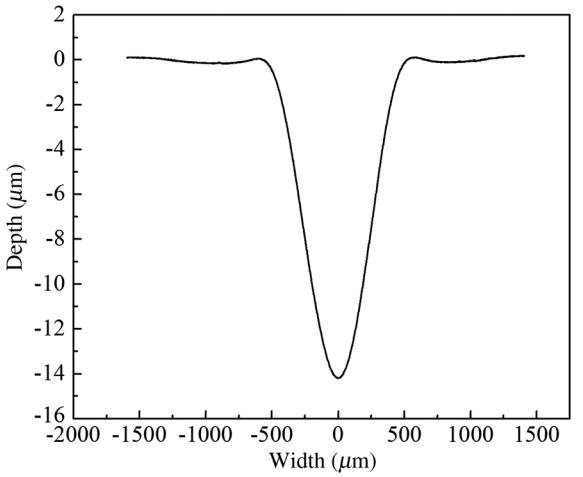

Fig. 6 Stylus profilometry (Ambios XP-Plus 300) traces of the crater created by the CO_2 laser beam.

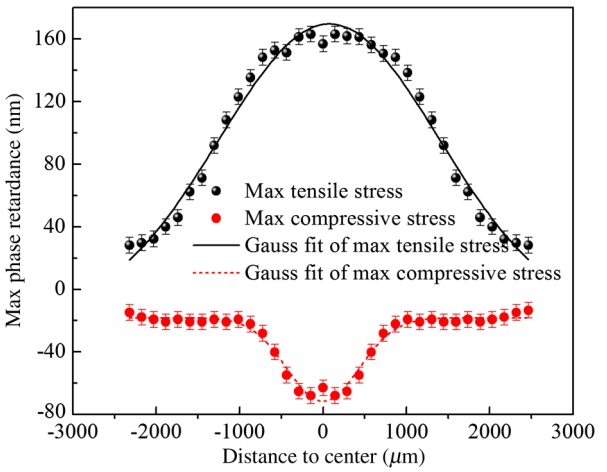

Fig. 7 The distribution of the maximum phase retardation induced by axial stress along the radials.

In this paper, for the Gaussian shape of the CO_2 laser beam, the light intensity in the beam center is much higher than that in the surrounding region. Because of the surface tension gradients and vapor recoil pressure effects during laser heating and cooling, those molten materials could redistribute.[18] Consequently, a near Gaussian crater is formed at the center of the irradiated region. Because both plastic and elastic deformations accompany the formation of the crater, both the maximum of the tensile and the compressive stresses are near Gaussian distribution in the irradiated zone.

4 Conclusion

The residual stress distribution of fused silica induced by CO_2 laser irradiation was characterized with two methods: the Senarmort compensated method and the sensitive color method. The experimental results show that the maximum phase retardance induced by hoop stress appears at the boundary of the laser distorted zone (680-μm distance to the center) and its value reaches 30 nm, but the hoop stress decreases rapidly and linearly inward, and decreases slowly and exponentially outward. For the axial stress along the depth direction, tensile stress lies in a thin surface layer (<280 μm) and compressive stress lies just below the tensile region. The maximum phase retardance induced by axial tensile stress is located at 50 to 100 μm below the surface, and its value reaches 150 nm. The maximum phase retardation caused by axial compression stress is located at the depth of 320 μm from the surface, and its value is about 75 nm. In addition, the distribution of the maximum axial stress is near Gaussian.

Acknowledgments

This paper is financially supported by the National Natural Science Foundation of China (Grant No. 61178018) and the PhD Funding Support Program of Education Ministry of China (Grant No. 20110185110007).

References

1. J. H. Campbell et al., "NIF optical materials and fabrication technologies: an overview," *Proc. SPIE* **5341**, 84–101 (2004).
2. M. D. Feit et al., "Statistical description of laser damage initiation in NIF and LMJ optics at 355 nm," *Proc. SPIE* **3492**, 188–195 (1999).
3. H. S. Peng et al., "Design of 60-kJ SG-III laser facility and related technology development," *Proc. SPIE* **4424**, 98–103 (2001).
4. H. Bercegol et al., "The impact of laser damage on the lifetime of optical components in fusion lasers," *Proc. SPIE* **5273**, 312–324 (2004).
5. S. G. Demos, M. Staggs, and M. R. Kozlowski, "Investigation of processes leading to damage growth in optical materials for large-aperture lasers," *Appl. Opt.* **41**(18), 3628–3633 (2002).
6. B. Bertussi et al., "Initiation of laser-induced damage sites in fused silica optical components," *Opt. Express* **17**(14), 11469–11479 (2009).
7. L. W. Hrubesh et al., "Methods for mitigating surface damage growth in NIF final optics," *Proc. SPIE* **4679**, 23–33 (2002).
8. E. Mendez et al., "Localized CO2 laser damage repair of fused silica optics," *Appl. Opt.* **45**(21), 5358–5367 (2006).
9. M. Matthews et al., "Residual stress and damage-induced critical fracture on CO2 laser treated fused silica," *Proc. SPIE* **7504**, 750410 (2009).
10. F. Guignard, M. L. Autric, and V. Baudinaud, "Temperature and residual stress evolution in CO2 laser irradiated glass," *Proc. SPIE* **3343**, 534–545 (1998).
11. P. A. Temple, W. H. Lowdermilk, and D. Milam, "Carbon dioxide laser polishing of fused silica surfaces for increased laser-damage resistance at 1064 nm," *Appl. Opt.* **21**(18), 3249–3255 (1982).
12. W. Dai et al., "Surface evolution and laser damage resistance of CO2 laser irradiated area of fused silica," *Opt. Lasers Eng.* **49**(2), 273–280 (2011).
13. T. D. Bennett and L. Li, "Modeling laser texturing of silicate glass," *J. Appl. Phys.* **89**(2), 942–950 (2001).
14. R. M. Vignes et al., "Thermomechanical modeling of laser-induced structural relaxation and deformation of glass: volume changes in fused silica at high temperatures," *J. Am. Ceram. Soc.* **96**(1), 137–145 (2013).
15. L. Gallais, P. Cormont, and J.-L. Rullier, "Investigation of stress induced by CO2 laser processing of fused silica optics for laser damage growth mitigation," *Opt. Express* **17**(26), 23488–23501 (2009).
16. Y. Jiang et al., "Characterization of 355 nm laser-induced damage of mitigated damage sites in fused silica," *Laser Phys.* **23**(2) (2013).
17. L. Yang et al., "Bulk damage and stress behavior of fused silica irradiated by nanosecond laser," *Opt. Eng.* **53**(4), 047103 (2014).
18. M. Feit et al., "Densification and residual stress induced by CO2 laser-based mitigation of SiO2 surfaces," *Proc. SPIE* **7842**, 78420O (2010).

Liang Yang is working toward his PhD in optics from the University of Electronic Science and Technology of China. His research interest is interaction between high-power lasers and optical materials.

Biographies of the other authors are not available.